Hindawi
Advances in Materials Science and Engineering
Volume 2022, Article ID 2652020, 9 pages
https://doi.org/10.1155/2022/2652020

Research Article

Phase-Change Materials, 1/*f* Noise, and Phase Synchrony

J. C. Martinez and R. E. Simpson

Singapore University of Technology and Design, 8 Somapah Road, 487373, Singapore

Correspondence should be addressed to J. C. Martinez; avecrux5@gmail.com

Received 25 August 2022; Revised 1 November 2022; Accepted 3 November 2022; Published 22 November 2022

Academic Editor: Zhigang Zan

In this article, we study $1/f^c, c \approx 1$ electrical noise in amorphous phase-change materials. Given the relevance of noise in recent applications, it is necessary to gain a deeper perspective on its nature in phase-change semiconductors, a promising class of materials. Electron conduction is envisaged in terms of an envelope function and a field-dependent Bloch wave function; the electron transport across the structure is modeled as driven phase oscillators under a weak field and obeys a Kuramoto-type equation. Its solutions naturally divide into a phase-synchronized group and phase-desynchronized oscillators. The former is comprised by long-lived pairs or aggregates and are responsible for $1/f, c = 1$ noise. We identify the dividing frequency between $\gamma = 1$ noise and $\gamma \neq 1$ noise. The phase-desynchronized carriers generate $\gamma \neq 1$ noise and are single carriers, not aggregates, and are short-lived. We apply our analysis to recent experiments.

1. Introduction

The discreteness of charge naturally implies fluctuations in electric power. Thus, a time-averaged value offers less information than the measurement in time. But might pairs or aggregates of discrete charges show up in these measurements [1, 2]? Such a phenomenon would be especially relevant for amorphous phase-change materials (PCMs), whose short-range order replaces the long-range order in crystals. For them, Anderson's negative-U (negative correlation) model suggests that, through the electron-lattice interaction and consequent lattice deformation, identical charges at the same site attract, notwithstanding their strong Coulomb repulsion [3]. It would then be interesting to see how this shows up in the context of $1/f$ flicker noise, which dominates the low-frequency region. Noise is important today due to its relevance to gravitational wave detection [4], Casimir torque experiments [5], and infrasound detection [6], among others. On the technological front, noise impacts the integrity of stored data, and for multibit phase-change devices, about 80% of the noise originates from current fluctuations [7].

Over sixty years ago, Ovshinsky announced the discovery of ovonic switching in amorphous materials [8]. That discovery was initially bypassed, but 60 years later, threshold switch selectors promise to transform data storage, in-memory computing, hardware neural networks, and other technologies [9]. An issue underpinning amorphous materials concerns the nature of electrical transport [10, 11]. Efforts to understand it have been in earnest over the past 20 years. Conduction in PCMs, to which chalcogenide alloys belong, has two disparate manifestations: when the material is amorphous, the resistance is very large; when the material is crystalline, the resistance drops by orders of magnitude. Conduction in the crystalline case can be explained in terms of those of a doped semiconductor with a small band gap and Fermi level lying near the valence band [12]. The amorphous allotrope, however, hosts many localized states that aid conduction only in the presence of large external electric fields [13, 14].

For semiconductors, noise measurements provide information about internal structure and device architecture [15]. Furthermore, low-frequency noise is a diagnostic for the quality of electronic devices [16], lending insight into processes in noncrystalline materials [17]. Aggregation could be a manifestation of phase synchrony among mobile electrons, with short-range order in PCMs constraining the extent of clustering.

At the beginning of the century, Pellegrini outlined an approach that foreshadows our picture of $1/f$ noise [18]. Even during the days of vacuum tubes, it was understood that $1/f$ noise consisted of a superposition of electron emission processes with a (roughly) uniform distribution of relaxation rates [19, 20]. Thus, only processes exhibiting an autocorrelation in time lead to $1/f$ noise. Presently, three approaches sum up the wisdom of the past decades. Beneventi et al. suggested a two-level model connecting two structural and electronic configurations with their associated bond lengths and angles in an amorphous lattice, thereby accounting for the variability of the trap energy and the population fluctuation of carriers [21]. Nardone et al. presented a two-state system of carriers of atomic or electronic nature in traps deep in the mobility gap [1]. They found the coupling between trap and double-well potential dominant enough to cause a large modulation of carrier concentration. Dmitriev et al. traced $1/f$ noise to fluctuations of the level occupancy of tail states near the conduction/valance band edges [22]. Aggregates in the context of $1/f$ noise were studied by Burin et al. [2] in connection with hopping conduction, which Nardone et al. showed to be inapplicable in PCMs [1]. We limit ourselves to amorphous PCMs because their short-range characteristic is unique to them. Importantly, this feature permits us to steer away of the controversy over the causes of $1/f$ noise.

The exponent of frequency for the $1/f$ noise spectral density as a function of frequency is not generally unity, though close. We will see instances of this shortly. Our focus is on this exponent γ hence, $1/f^{\gamma}$. One notices that γ tends to be less than unity as frequency grows. We show that $\gamma = 1$ occurs for aggregates and are in phase synchrony with each other. We refer to this as true $1/f$ noise, without prejudice to the rest. This circumstance is not inconsistent with Anderson's negative-U hypothesis [3].

In the following, we discuss the nature of the wave function for electron propagation in a crystal subject to an electric field, which serves as a local version of the same phenomenon in PCMs, at least for the extended states [23]. An important step is to identify the phase of the carrier in terms of its energy in a weak electric field. We then connect this discussion with phase oscillators, for which phase synchrony occurs. At this point, we are ready to appreciate the role that tail states in PCMs might hold for noise. We identify long-lived tail states as the carriers responsible for true $1/f$ noise and indicate how pairs/aggregates of charges can be long-lived. Finally, the discussion on phase oscillators is expanded to explain how $1/f$ noise depends on material thickness, as observed recently [24].

For recent applications of PCMs, we refer to the following reviews [25].

2. First Approach

Typically, $1/f$ noise in an electronic device accompanies the change in carrier trapping and detrapping, which manifests as temporal fluctuations [26]. In the case of amorphous chalcogenide PCMs, noise has been attributed to bond length/angle induced fluctuations of the mean trap energy [21]. As a first approach, we take the power spectral noise density due to a random signal, which was given by Machlup [27].

$$\phi(\omega) = \frac{1}{\pi}\frac{\sigma\tau}{(\sigma+\tau)^2}\frac{(1/\tau + 1/\sigma)}{\omega^2 + (1/\tau + 1/\sigma)^2}, \tag{1}$$

where σ and τ are trap emission and capture times and $f = \omega/2\pi$ the frequency. It describes a purely random signal in which emission and capture by traps are uncorrelated. The average power $\Phi(\omega)$ is found by integrating equation (1) successively over σ and τ through their distribution laws. Assuming a uniform distribution of trap depths, one has the distribution laws $p(\sigma) = (1/\ln\sigma_2/\sigma_1)1/\sigma$ and $p(\tau) = (1/\ln\tau_2/\tau_1)1/\tau$, where $\sigma_{1,2}$ and $\tau_{1,2}$ are largest and smallest values of these time parameters, this leads to [28]

$$\begin{aligned}\Phi(\omega)\&9;= {} & \frac{1}{\ln\sigma_2/\sigma_1}\frac{1}{\ln\tau_2/\tau_1}\frac{1}{2\pi\omega^2}\left\{\sum_{i=1,2}\sum_{j=1,2}(-)^j\left(\frac{1}{\sigma_j}+\frac{1}{\tau_i}\right)\log\frac{\left(\tau_i+\sigma_j\right)^2}{\sigma_j^2\left(1+\omega^2\tau_i^2\right)+2\tau_i\sigma_j+\tau_i^2}\right\} \\ \&9;\quad & +\frac{1}{\ln\sigma_2/\sigma_1}\frac{1}{\ln\tau_2/\tau_1}\frac{1}{\pi\omega}\left\{\tan^{-1}\frac{\omega\sigma_2^2\tau_2-\tau_1)}{\tau_2\tau_1\left(1+\omega\sigma_2^2\right)+\sigma_2\tau_2+\sigma_2\tau_1+\sigma_2^2}-\tan^{-1}\frac{\left(\omega\sigma_1^2\tau_2-\tau_1\right)}{\tau_2\tau_1\left(1+\omega\sigma_1^2\right)+\sigma_1\tau_1+\sigma_1\tau_2+\sigma_1^2}\right\},\end{aligned} \tag{2}$$

which shows $1/f$ and $1/f^2$ components. The noise power is symmetric with respect to interchange of $\sigma_{1,2}$ and $\tau_{1,2}$. For amorphous materials, the log terms are effectively negligible so only the arctangent terms are important. This then gives us the $1/f$ flicker noise power.

Figure 1 compares equation (2) with spectral noise power, $S = I^2\Phi(\omega)$, measurements for a-GeTe at room temperature, using Au and Mo electrodes [29]. We see agreement between the data and equation (2) starting to fray for frequencies beyond $\sim 10^2$ Hz. Above this threshold frequency, the exponent $\gamma = 0.9$ becomes appropriate as suggested by the short black line in Figure 1. More recent measurements by Beneventi et al. [30] for PCMs exhibit a similar trend and roughly similar threshold frequencies. The effect is also seen in amorphous materials such as a-Si: H and nanocrystalline-Si: H thin-film transistors [31].

The above development reasonably captures the general mechanism for noise but requires additional new input to

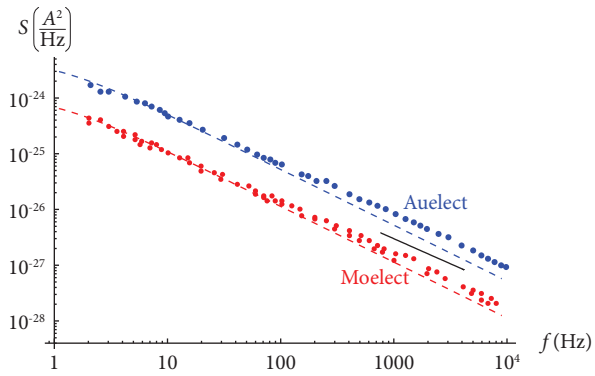

FIGURE 1: Room temperature data for GeTe [29] compared with equation (2) (blue and red lines): $\sigma_1 = 10^{-6}$ s, $\sigma_2 = 2.5$ s and $\tau_1 = 10^{-6}$ s, $\tau_2 = 2.5$ s. A $1/f^{0.9}$ line in black is shown at the bottom right of the graph for comparison.

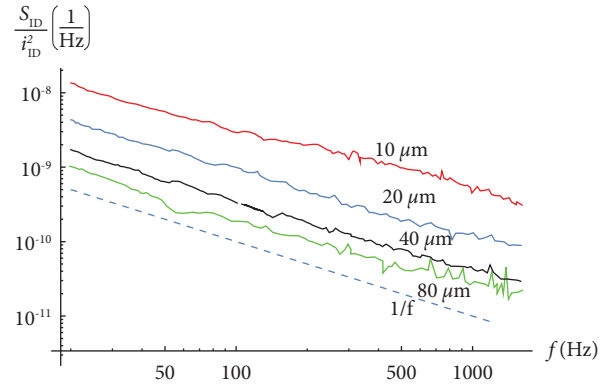

FIGURE 2: Normalized drain-current noise spectral densities (S_{ID}/I_{ID}^2) for four channel thicknesses of amorphous indium-gallium-zinc-oxygen thin film transistors [24]. Dashed line at bottom represents a $1/f$ line.

confront more recent observations. An example is the measurement by Lee et al. of the noise spectral densities of amorphous indium-gallium-zinc-oxygen thin film transistors [24]. Figure 2 shows a decreasing spectral density as the thickness increases, which is unexplained by equation (2).

3. Introducing the Kuramoto Equation

In studies of electron propagation in 1D in a crystal subjected to a constant field $\mathscr{E}$, the potential (Figure 3) is decomposed into a part that shares the lattice periodicity and a portion that does not. The latter has zero matrix elements with the energy-band states associated with the combined periodic crystal potential and periodic part of the potential [32]. In the absence of scattering, an electron can be described in terms of a field-dependent Bloch wave with an associated field-dependent phase. For such an electron with wave number k_0 at time $T = 0$, the wave function at time T is [32]

$$\Psi(x,T) = e^{ik_0 x} u_{n,k_0+q\mathscr{E}T/\hbar}(x) \exp\left(\frac{i}{q\mathscr{E}} \int_{k_0}^{k_0+q\mathscr{E}T/\hbar} \epsilon(k',\mathscr{E})dk'\right), \tag{3}$$

$\epsilon(k,\mathscr{E})$ is the energy eigenvalue for fixed wave number k, $u_{n,k}(x)$ an electric-field-dependent Bloch state (n = band index) and the time-dependent phase comes from the nonperiodic portion. Solution (3) has the period $\hbar/ea\varepsilon$, a = lattice spacing and generalizes to many bands. Although the crystalline environment differs from that of the amorphous, locally the two are similar [13, 14, 23]. Thus, we assume that charge carriers in the amorphous material can also be described locally by equation (3). The phase ϕ has the time derivative $\dot{\phi} \approx \omega + \epsilon(k,\varepsilon)/\hbar$. $\epsilon(k,\mathscr{E})$ is available in the literature [33, 34]. In the tight-binding approximation it can be written as $\epsilon(k,\varepsilon) = -2t \sin(ka - \eta)$, t being the transfer energy for nearest-neighbour hopping and η is a small phase [34] (T is time). Recognizing ka as the natural expression for phase we write

$$\dot{\phi} \approx \omega - \frac{2t}{\hbar} \sin(\phi - \eta). \tag{4}$$

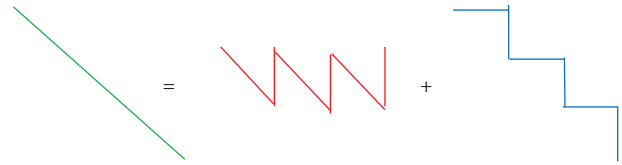

FIGURE 3: In a crystal, (a) the linear external electric potential can be broken into (b) its periodic saw-tooth component and (c) its nonperiodic staircase-like component.

Equation (4) has the form of the Kuramoto equation, which pervades studies of the synchronized behavior of coupled oscillators [35]. There ϕ is viewed as a collective variable describing the phases of a large number of oscillators, ϕ_i, $i = 1, \ldots, N$, with phases ϕ_i, natural frequencies ω_i and instantaneous frequencies $\dot{\phi}_i$:

$$\dot{\phi}_i = \omega_i + \frac{K}{N} \sum_{j=1}^{N} \sin(\phi_j - \phi_i). \tag{5}$$

K being the coupling strength. The average phase of the collection, Φ, is defined through an order parameter.

$$Z = \frac{1}{N} \sum_{i=1}^{N} e^{i\phi_i} = re^{i\Phi}. \tag{6}$$

r being the amplitude, using equations. (5) and (6) one derives equation (4) where Kr is replaced by $2t/\hbar$ It is convenient to regard K as the interaction coupling while $r(T)$ $\in [0,1]$ is interpreted as a measure of phase coherence or degree of synchrony. If all oscillators move in phase, then $r = 1$; if the phases are scattered and no recognizable rhythm prevails, $r \approx 0$. An individual oscillator satisfies $\dot{\phi}_i \approx \omega_i - Kr \sin(\phi_i - \Phi)$.

Although ϕ_i appears superficially to be uncoupled from the rest, all the oscillators are really interacting through the mean-field quantities r and Φ. Studies, confirmed by simulations, suggest that phase ϕ_i is pulled toward Φ rather than to any individual ϕ_j [35]. Intuitively, this implies more oscillators tending toward Φ and to growing synchrony,

thereby increasing r and Kr and drawing yet more oscillators into synchrony. A feedback loop between coupling and synchrony thus sets in. One now goes to a frame rotating with angular velocity Ω ($= \dot{\Phi}$). Then, the equation for $\dot{\phi}$ can be written as

$$\dot{\phi} \approx \omega - \Omega - Kr \sin \phi. \tag{7}$$

Integration yields two solutions: for $|\omega - \Omega| \leq Kr$, the system has a stable fixed point at

$$\phi^* = \arcsin\left(\frac{\omega - \Omega}{Kr}\right). \tag{8}$$

For $|\omega - \Omega| > Kr$, the system has no fixed point ([35], see also supplementary material [36]) The first consists of synchronized oscillators with phases locked at ϕ^* and entrained in the rotating frame. The second corresponds to oscillators with no equilibrium solution; they remain unlocked and drift nonuniformly. Kr ($2t/\hbar r$ in equation (4)) is the cut-off frequency dividing the synchronized from the unsynchronized oscillators. With increased synchrony, r grows and so does the cut-off frequency until $r = 1$ is reached, which is the steady state. Of course, a system may fall short of $r = 1$ and remain in that partially synchronized state. The phases of the desynchronized oscillators are periodic [37]. Having obtained the solution, one must check consistency with the order parameter. We will not pursue this (see [35]) but return to it for a related problem below.

4. Phase-Change Materials

Before proceeding further in our development, we pause to describe the properties of phase-change materials (PCMs), which will concern us primarily in the paper. The most popular PCMs are $Ge_2Sb_2Te_5$ (GST) and GeTe. Besides their periodicity, crystals are endowed with distinct conduction and valence bands that are well separated in energy. In amorphous materials, on the other hand, the periodicity is replaced by a short-range order and, despite the loss of periodicity, there may still be a considerable degree of ordering locally [13, 14]. A universal feature of amorphous materials is the presence of band-tail states, that is, localized electronic states populating the energy region below the conduction band and above the valence band [38]. These states dominate the conduction properties of these materials. The existence of these band states is usually attributed to disorder, whether thermal, structural, compositional, or arising from impurities.

Remarkably the band-tail states are well described by an exponential distribution with a characteristic energy ε_0 [38, 39]. Thus, the density of states of these tail states falls exponentially inside the band gap (since we are in the gap, energy ε has a negative sign) [40]

$$\rho(\varepsilon) = \rho(0) e^{\varepsilon/\varepsilon_0}. \tag{9}$$

The relaxation time τ associated with a single fluctuation is distributed across a large energy interval by

$$\tau(\varepsilon) = \tau(0) e^{-\varepsilon/\varepsilon_1}. \tag{10}$$

In which ε_1 is the characteristic energy for capture. This dependence can be explained through the multiphonon capture mechanism ([41, 42]; also sec. IV C. 2 of [1]). Note, that the symbol τ here is not the same as a similar quantity introduced in equation (2). We see from equation (10) that long relaxation times correspond to large $\varepsilon/\varepsilon_1$. The above features of PCMs naturally provide the requisite autocorrelation noted earlier.

The exponential distribution of relaxation times is a basic feature of PCMs [38], and relaxation times spanning the range from picoseconds to years are not new [43]. An estimate of the activation relaxation time for PCMs for the electronic double-well potential due to a pair of negative-U centers is [1].

$$\tau = \tau_{\min} \exp\left[\frac{2R}{a} + \frac{\Delta W_B(R)}{k_B T}\right], \tau_{\min} = \tau_0 \exp\frac{W_B(R_{\min})}{k_B T}, \tag{11}$$

where R = intercenter separation, $\Delta W_B(R) = W_B(R) - W_B(R_{\min})$, a = electron localization radius, $\exp[2R/a]$ accounts for electron tunneling, $\tau_0 \sim 10^{-12}$ as the atomic vibration time. With typical parameters $a \sim 10^{-9}$m, $R \sim 10^{-8}$m, $\Delta W_B \sim 1$eV [1], one obtains $\tau_{\min} \sim 10^{-4}$ s and $\tau \sim 10^{17}$ s. Although rough, the estimates point to the existence of very long relaxation times. If this is true with pairs it is especially true with aggregates.

Long-lived states are characterized by large W_B. In the context of pairs, this in turn occurs when electrons are widely separated [1]. Long-lived states are also associated with a heavy polaron cloud accompanying atomic deformation [1]. The reverse holds for closely separated pairs which are usually referred to as intimate pairs. In the case of aggregates, i.e., many electrons loosely forming a pack, the corresponding W_B would be large, and such a pack is long-lived on account of the many phonons playing a role akin to photons mediating between electrons. Long-lived electronic states are hardly new; they have also been invoked in studies of resistance drift in spin glasses, disordered superconductors, granular materials, colloids, and similar systems [44], where they originate from structural relaxation. Since McWhorter's work [45], it is common to associate long-lived states with surface traps and contacts ([40], p722) but the view that even bulk traps can be long-lived has gained traction currently [46]. Indeed, equation (11) does not suggest any special distinction between surface and deep traps.

For amorphous PCMs, we envisage conduction in terms of classical electrons being thermally emitted and hopping over the top of the Coulomb-barrier humps between donor-like traps separated by a potential hump created by the Coulomb potential between the two adjacent traps. See Figure 4. This is the Poole–Frankel (PF) picture [47]. For guidance, consider a-GeTe. Its carrier density is $\sim 10^{24}\,\mathrm{m}^{-3}$, implying spacing between carriers/traps of ~ 10 nm, assuming no pairs or aggregates [48]. The Coulomb repulsive energy for two electrons $a = 2.7$ nm apart is $e^2/\epsilon a \approx 10$ meV,

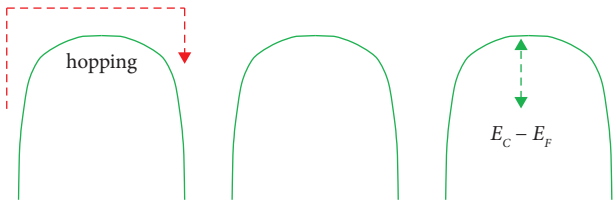

FIGURE 4: In red, the PF picture of electron hopping between traps originating from potential humps created by the Coulomb interaction between trapping centers. The barrier height $E_C - E_F$ is the potential difference between the conduction band and Fermi level.

where the dielectric constant $\epsilon \approx 25$ [49] is used. For a Hubbard energy $U \sim -0.5$ eV [50], this implies ~ 50 pairs of electrons can be supported between successive traps. These are the clusters or aggregates.

5. 1/*f* Noise in PCMs

We saw above that despite the fact that Machlup's noise density (4) captured the basic physics of noise, it failed to explain the thickness dependence of more recent experimental data. To his basic picture of random telegraph signals, we must now include also the feature of band-tail relaxation discussed above. Copeland [51] wrote the square of the rms noise current i as

$$\frac{\langle i^2 \rangle}{\Delta f} = \frac{2\tau I^2}{n^2 V} F(1-F) \frac{1}{1+(\omega\tau)^2}. \tag{12}$$

$F = (1/1 + e^{-\beta(\varepsilon_F - \varepsilon)})$ being the Fermi–Dirac distribution, V sample volume, n = concentration of carriers, $\beta = 1/k_B T$, T = temperature and I current. The relative spectral noise density dS for electron number fluctuations induced by occupancy fluctuations in the energy interval $d\varepsilon$ [22] is

$$dS(\varepsilon) = \rho(\varepsilon) \frac{2I^2 \tau(\varepsilon)}{n^2 V} \frac{F(1-F)}{1+\omega^2 \tau(\varepsilon)^2} d\varepsilon. \tag{13}$$

Integration over energies yields the spectral noise density. We approximate F with unity and $1 - F$ with $e^{-\beta(\varepsilon_F - \varepsilon)}$. To obtain a frequency-dependent result the term $\omega^2 \tau(\varepsilon)^2$ in the denominator cannot be neglected. Since we are only interested in frequency dependence, we extract it upon employing appropriate substitutions and find that the noise spectrum is proportional to $f^{-1+1+\nu_0/\nu_1}$, where $\nu_1 = kT/\varepsilon_1, \nu_0 = kT/\varepsilon_0$ [1, 22]. Typically, ε_1, kT and ε_0 are in the meV range (for GeTe they are, respectively, 13 [52], 26, and 89 [53] meV), and we see why the exponent of f is not −1. However, if the carriers are pairs or aggregates of charges, instead of just single charges, and then, $\nu_1 \gg 1$. Thus, for aggregates we expect the exponent of f to be effectively 1.

We can now combine this discussion with that on phase synchrony. Noise below the cut-off frequency originates from carriers moving with a common phase. As we saw, they form aggregates, are long-lived since $\nu_1 \gg 1$. Their flicker noise has the exponent $\gamma = 1$, i.e., they emit true $1/f$ noise. We can employ an analogy to understand this. Envisaging carriers as masses linked by springs, total energy scales with the number N of masses (each of mass m) while frequency is inversely proportional to N. To see this latter result, recall that the equivalent stiffness for N springs in series is k/N, k being individual stiffness; frequency is proportional to the square root of effective stiffness divided by mass, i.e., $\sqrt{k/N/Nm}$. The product of energy and its frequency is constant, explaining why this noise scales as $1/f$. Charges emitting noise at frequencies above the cut-off drift with random phases and shorter lifetimes. For them $\nu_1 \sim O(1)$ and $\gamma < 1$. They do not form aggregates and move as individual charges. They are further apart while the synchronized group is mobile aggregates. Aggregates are massive and generate more noise than individual drifters.

To estimate the transfer energy for a-GeTe, which is given by $t = \hbar^2/2ma$ where m is mass and a is separation [54], we start with the value for graphene, which is 2.4 meV [55]. This is of course for a crystal; we have to find the equivalent value for amorphous PCMs. Recall that we saw how ~ 50 pairs of electrons can aggregate in one direction. In 3D then, we have 10^6 electrons in a packed cluster. The hopping distance is now of order 10 nm [10] compared with a spacing in graphene of $a \sim 2$Å. This leads to an estimate of $t \sim 10^{-12}$ eV corresponding to a frequency of around 200 Hz (see also supplementary material [36]). This is our cut-off frequency for PCMs, which matches observations mentioned above.

In Figure 2 we saw that $S(\varepsilon)/I^2$ generated by a thinner PCM is greater than that of a thicker one. This had been attributed to carriers hopping across more traps in thicker materials, leading to stronger averaging on the noise [56]. However, the impact of averaging upon the carriers is unclear. Here, we attempt a simplified approach. We look upon hopping as an external periodic force near a mean frequency. Equation (5) is modified by adding on the right-hand side a term $b \sin(\omega_f T - \phi_i)$, where ω_f (b) is the frequency (strength) of the force [57]. Since equation (5) has units of inverse time, "external force" is used here analogically. The Kuramoto equation is now

$$\dot{\psi}_i = \omega_i - \omega_f - b' \sin(\psi_i - \psi_0). \tag{14}$$

The order parameter is $Z = 1/N \sum_{i=1}^{N} e^{i\phi_i} = re^{i(\phi_0 + \omega_f T)}$. The Kuramoto equation then takes the form

$$\dot{\psi}_i = \omega_i - \omega_f - b' \sin(\psi_i - \psi_0), \tag{15}$$

where $\psi_i = \phi_i - \omega_f T$, $\tan\psi_0 = K\sigma \sin\phi_0/(b + K\sigma\cos\phi_0)$, $b' = \sqrt{b^2 + K^2 r^2 + 2Krb\cos\phi_0}$. Solutions are

$$\psi_i = \psi_0 + \sin^{-1}\frac{\omega_i - \omega_f}{b'}, \left|\frac{\omega_i - \omega_f}{b'}\right| \leq 1 \text{synchronize d group}, \tag{16a}$$

$$= \tilde{\omega}_i T + \psi_0 + h(\tilde{\omega}_i T), \left|\frac{\omega_i - \omega_f}{b'}\right| > 1 \text{ de synchronize d group}. \tag{16b}$$

with $\tilde{\omega}_i = \sqrt{(\omega_i - \omega_f)^2 - b'^2} > 0$. $h(x)$ is a function with the period 2π [36, 58]. These generalize solutions of equation (7).

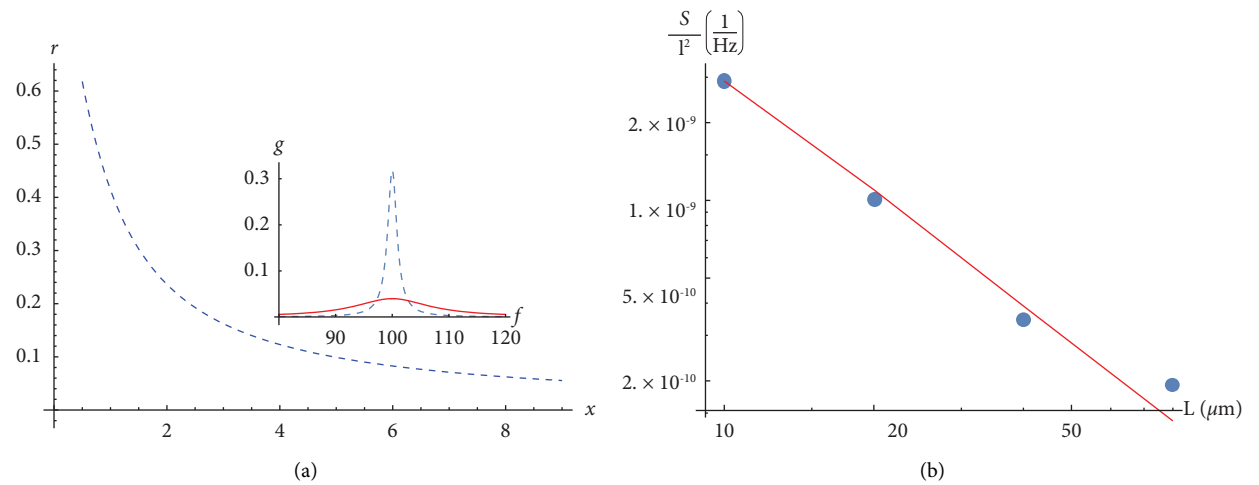

FIGURE 5: (a) r versus x, displaying decrease in synchrony with x. Inset shows Lorentz distribution for two values of Γ: Γ = 1 (black, dashed), 8 (red, solid) exhibiting increased frequency spread in the latter. (b) Comparison between the consistency analysis and data for a-IGZO shown in Figure 2 for frequency 100 Hz [24].

We check self-consistency assuming r and ϕ_0 are time-independent. For $N \longrightarrow \infty$, the system of phase oscillators is described in terms of a probability distribution $\rho(\psi \mid \omega)$ where $\rho(\psi \mid \omega)d\psi$ gives the fraction of oscillators with phase between ψ and $\psi + d\psi$ for frequency ω. The order parameter is expressed as

$$re^{i\phi_0} = \int_0^{2\pi} d\psi\, \rho(\psi) e^{i\psi} = \int_{-\infty}^{\infty} d\omega\, g(\omega) \int_0^{2\pi} d\psi\, \rho(\psi \mid \omega) e^{i\psi}. \tag{17}$$

$g(\omega)$ being the distribution of oscillator frequencies. From equation (16a), the synchronized oscillators obey

$$\rho_s(\psi) = g(\omega)\frac{d\omega}{d\psi} = g\left(\omega_f + b' \sin(\psi - \psi_0)\right) b' \cos(\psi - \psi_0), \left|\psi - \psi_0\right| \leq \frac{\pi}{2}. \tag{18a}$$

For the desynchronized group, more effort is required [36, 57]:

$$\rho_{ds}(\psi) = -\frac{b'}{2\pi} \int_{|\omega| > b'} \frac{\cos\theta}{\sin^2\theta} d\theta\, g\left(\omega_f + \frac{b'}{\sin\theta}\right) \frac{\sqrt{1 - \sin^2\theta} - 1}{1 - \sin\theta \sin\psi}, \tag{18b}$$

and equation (17) yields the consistency equation

$$re^{i\phi_0} = b' \left\{ \int_{-\pi/2}^{\pi/2} d\psi\, g\left(\omega_f + b' \sin\psi\right) \cos\psi e^{i\psi} - iH \right\}, \tag{19}$$

where $H = \int_0^{\pi/2} [(\cos^2\theta - \cos\theta)/\sin^3\theta] d\theta [g(\omega_f + b'/\sin\theta) - g(\omega_f - b'/\sin\theta)]$.

We assume a Lorentzian distribution centered around ω_f, $g(\omega) = (\Gamma/\pi)[1/((\omega - \omega_f))^2 + \Gamma^2]$, where parameter Γ is half the width at half the maximum height. Substituting into equation (17) we obtain $re^{i\phi_0} = (2\Gamma/\pi)b' \int_0^{\pi/2} d\psi 1/\left\{b'^2 \sin^2\psi + \Gamma^2)\cos^2\psi\right\}$. Other terms vanish due to symmetry. In this simplified model, the order parameter is real and we find

$$r = \sqrt{1 + x^2} - x, x = \frac{\Gamma}{b'}. \tag{20}$$

This is our consistency requirement. As noted above, r is a measure of synchrony and below a frequency of ~ 200 Hz it is also a measure of the number of particles and hence, noise density. To relate this to our problem we study the scaling properties of Γ and b'. As length L increases so does Γ , that is, the range of significant frequencies of $g(\omega)$ grows linearly (see Figure 5(a)). On the other hand, b' decreases with length. Indeed, as L grows so does barrier height, an effect attributed to the percolative nature of the conduction mechanism [58, 59]. Intuitively, larger length implies more hopping which diminishes driving strength b'. We assume $b' \sim 1/\sqrt{L}$, and obtain the dependence, $x \sim L^{3/2}$. Figure 3 suggests that the weakening of the driving force with increased length coupled with increased spectral frequency spread are the factors responsible for the decrease in the noise density in PCM. Figure 5(b) shows $S(\varepsilon)/I^2$ versus length for a-IGZO data from Figure 2 at the frequency 100 Hz (see supplementary material [36] for more detail). The agreement between the prediction (curve) and data points is reasonable. Very similar results were also obtained by Jeyasingh et al. [56] for GST. Moreover, a result supporting a similar conclusion but for graphene, which is not a PCM but crystalline, has also been reported [60]. Although an abundance of data is still unavailable, the latter observation points to a trend applicable to $1/f$ noise for materials beyond the realm of PCMs.

A question that has baffled researchers is whether $1/f$ noise is found at equilibrium [61]. Under thermal equilibrium there should be no current, hence, no noise. Herein, we answer by going back to equation (4) and the energy $\epsilon(k, \varepsilon)$. The result for $\epsilon(k, \varepsilon)$ is rigorously correct provided $t/\mathcal{N}e\varepsilon a \gg 1$, $\mathcal{N}$ = number of lattice sites [34]. As the field ε

approaches zero, the tight-binding result for energy becomes exact and we can expect equation (4) to hold rigorously. In the context of PCMs, the rest of the argument stands and we should be able to observe $1/f$ noise in the limit $\varepsilon \longrightarrow 0$, i.e., as thermal equilibrium is approached.

Our objective in this paper was to identify the source of true $1/f$ noise which we traced to the long-lived tail states. If $1/f$ noise is to be minimized, we found that, by far, the most important source of that noise lies in the low frequency regime, which corresponds to the long-lived states. Higher frequency contributions to the spectral density decay exponentially with frequency. Therefore, ways of eliminating the contribution from long-lived states would go far in reducing the undesirable effects of noise in electronic devices, whether amorphous or crystalline. This is also the first time that phase synchrony is associated with $1/f$ noise and, while there appear to be many factors responsible for this type of noise, the role of phase in this context is well worth further study.

6. Conclusions

In summary, we studied $1/f^{\gamma}$ noise, where, $\gamma \approx 1$, in amorphous PCMs. Guided by a description of electron conduction in terms of an envelope function and field-dependent Bloch wave function, we modeled electrons as driven phase oscillators and obtained a Kuramoto-type equation for their phase under a weak field. This equation yielded solutions describing phase-synchronized and phase-desynchronized oscillators. We identified the former as being responsible for true $1/f, \gamma = 1$ noise. They are long-lived aggregates. We identified the dividing frequency between $\gamma = 1$ noise and $\gamma \neq 1$ noise. The phase-desynchronized carriers correspond to short-lived single carriers. Our findings help to understand recent experiments.

We acknowledge support from the Singapore Ministry of Education (project number MOE2017-T2-1-161) and the A-Star NSLM Program (project number: A18A7b0058). This work was carried out under the auspices of the SUTD-MIT International Design Center (IDC).

Data Availability

The data are available in the paper itself as well as in the supplementary information. Requests for the data can be addressed to the first author.

Conflicts of Interest

The authors declare that there are no conflicts of interest with respect to the research, authorship, and/or publication of this article.

Acknowledgments

The authors would like to thank Singapore Ministry of Education (project number (MOE2017-T2-1-161) and the A-Star NSLM Program (project number A18A7b0058).

Supplementary Materials

Supplementary material related to this paper is available along with it. It contains further details on most of the calculations given in the paper and additional details about Figure 5. (*Supplementary Materials*)

References

[1] M. Nardone, V. I. Kozub, I. V. Karpov, and V. G. Karpov, "Possible mechanisms for 1/f noise in chalcogenide glasses: a theoretical description," *Physical Review B: Condensed Matter*, vol. 79, no. 16, Article ID 165206, 2009.

[2] A. L. Burin, B. I. Shklovskii, V. I. Kozub, Y. M. Galperin, and V. Vinokur, "Many electron theory of1/fnoise in hopping conductivity," *Physical Review B: Condensed Matter*, vol. 74, no. 7, Article ID 075205, 2006.

[3] P. W. Anderson, "Model for the electronic structure of amorphous semiconductors," *Physical Review Letters*, vol. 34, no. 15, pp. 953–955, 1975.

[4] L. Yang, G. Vajente, M. Fazio et al., "Enhanced medium-range order in vapor-deposited germania glasses at elevated temperatures," *Science Advances*, vol. 7, no. 37, Article ID eabh1117, 2021.

[5] D. A. T. Somers, J. L. Garrett, K. J. Palm, and J. N. Munday, "Measurement of the Casimir torque," *Nature*, vol. 564, no. 7736, pp. 386–389, 2018.

[6] A. J. Bedard and T. M. Georges, "Atmospheric infrasound," *Physics Today*, vol. 53, no. 3, pp. 32–37, 2000.

[7] G. F. Close, U. Frey, M. Breitwisch et al., "Device, circuit and system-level analysis of noise in multi-bit phase-change memory," *IEDM Tech. Dig*, pp. 29.5.1–29.5.4, 2010.

[8] S. R. Ovshinsky, "Reversible electrical switching Phenomena in disordered structures," *Physical Review Letters*, vol. 21, no. 20, pp. 1450–1453, 1968.

[9] L. Hoddeson and P. Garrett, "The discovery of Ovshinsky switching and phase-change memory," *Physics Today*, vol. 71, no. 6, pp. 44–51, 2018.

[10] D. Ielmini, "Electrical transport in crystalline and amorphous chalcogenide," in *Phase Change Memory: Device Physics, Reliability and Applications*, A. Redaelli, Ed., pp. 11–40, Springer, Heidelberg, Germany, 2018.

[11] D. Ielmini and A. L. Lacaita, "Phase change materials in non-volatile storage," *Materials Today*, vol. 14, no. 12, pp. 600–607, 2011.

[12] D. Ielmini, "Unified physical modeling of reliability mechanisms and scaling perspective of phase change memory," *Current Applied Physics*, vol. 11, no. 2, pp. e85–e91, 2011.

[13] N. Mott and E. Davis, *Electronic Processes in Non-crystalline Materials*, Oxford Univ. Press, Oxford, UK, 1979.

[14] S. R. Elliot, *Physics of Amorphous Materials*, Longman Press, Harlow UK, 1983.

[15] A. Van Der Ziel, *Noise: Sources Characterization Measurement*, Prentice-Hall, Englewood Cliffs, NJ, USA, 1970.

[16] L. K. J. Van Damme, "Noise as a diagnostic tool for quality and reliability of electronic devices," *IEEE Trans. Electron Devices*, vol. 41, no. 11, pp. 2176–2187, 1994.

[17] M. B. Weissman, "Low-frequency noise as a tool to study disordered materials," *Annual Review of Materials Science*, vol. 26, no. 1, pp. 395–429, 1996.

[18] B. Pellegrini, "A general model of 1/fγ noise," *Microelectronics Reliability*, vol. 40, no. 11, pp. 1775–1780, 2000.

[19] W. Schottky, "Small-shot effect and flicker effect," *Phys. Rev.*vol. 28, no. 1, pp. 74–103, 1926.

[20] J. Bernamont, "Fluctuations de potentiel aux bornes d'un conducteur métallique de faible volume parcouru par un courant," *Ann. Phys. (Leipzig)*, vol. 11, pp. 71–140, 1937.

[21] G. B. Beneventi, A. Calderoni, P. Fantini, L. Larcher, and P. Pavan, "Analytical model for low-frequency noise in amorphous chalcogenide-based phase-change memory devices," *Journal of Applied Physics*, vol. 106, no. 5, Article ID 054506, 2009.

[22] A. P. Dmitriev, E. Borovitskaya, M. E. Levinshtein, S. L. Rumyantsev, and M. S. Shur, "Low frequency noise in degenerate semiconductors," *Journal of Applied Physics*, vol. 90, no. 1, pp. 301–305, 2001.

[23] R. A. Street, *Hydrogenated Amorphous Silicon*, Cambridge U. Press, Cambridge, UK, chap. 1, 1991.

[24] J.-M. Lee, W.-S. Cheong, C.-S. Hwang, I.-T. Cho, H.-I. Kwon, and J.-H. Lee, "Low-frequency noise in amorphous indium–gallium–zinc-Oxide thin-film transistors," *IEEE Electron Device Letters*, vol. 30, no. 5, pp. 505–507, 2009.

[25] Y. Kim, C. Kim, and M. Lee, "Parallel Laser Printing of a thermal emission Pattern in a phase-change thin film Cavity for Infrared Camouflage and security," *Laser & Photonics Reviews*, vol. 16, no. 3, Article ID 2100545, 2022.

[26] F. N. Hooge, "1/f noise sources," *IEEE Trans. Electron. Devices*, vol. 41, no. 11, pp. 1926–1935, 1994.

[27] S. Machlup, "Noise in semiconductors: spectrum of a two-parameter random signal," *Journal of Applied Physics*, vol. 25, no. 3, pp. 341–343, 1954.

[28] A. Stepanescu, "1/f noise as a two-parameter stochastic process," *Il Nuovo Cimento B Series 11*, vol. 23, no. 2, pp. 356–364, 1974.

[29] K. P. Sharnhorst, L. Demske, and G. M. Black, *The Noise Equivalent Power of Amorphous GeTe/SiOxTwo Color Detector*, Naval Surface Weapons Center, Silver Spring, Maryland/Tr-76-98, 1976.

[30] G. B. Beneventi, M. Ferro, and P. Fantini, "$\hbox{1}/f$ noise in 45-nm RESET-state phase-change memory devices: Characterization, impact on memory readout Operation, and scaling perspectives," *IEEE Electron Device Letters*, vol. 33, no. 11, pp. 1559–1561, 2012.

[31] E. G. Ioannidis, A. Tsormpatzoglou, D. H. Tassis, C. A. Dimitriadis, F. Templier, and G. Kamarinos, "Characterization of traps in the gate dielectric of amorphous and nanocrystalline silicon thin-film transistors by 1/f noise," *Journal of Applied Physics*, vol. 108, no. 10, Article ID 106103, 2010.

[32] D. Emin and C. F. Hart, "Existence of w," *Physical Review B: Condensed Matter*, vol. 36, no. 14, pp. 7353–7359, 1988.

[33] G. C. Stey, G. Gusman, and M. Saitoh, "Emergent Bloch Oscillations in a kinetically constrained rydberg spin lattice," *Journal of Physics C: Solid State Physics*, vol. 6, no. 4, pp. 650–656, 1973.

[34] H. Fukuyama, R. A. Bari, and H. C. Fogedby, "Tightly bound electrons in a uniform electric field," *Physical Review B: Condensed Matter*, vol. 8, no. 12, pp. 5579–5586, 1973.

[35] Y. Kuramoto, "Int. Symp. On mathematical problems in theoretical physics (Lecture notes in physics)," in *Proceedings of the International Symposium on Mathematical Problems in Theoretical Physics*, vol. vol 30, p. 420, Kyoto, Japan, January 1975.

[36] Supplementary Material accompanying this article: The Paper Is Complete without This Supplementary Material. However, it Does Contain More Detail and Explanation that the Reader Could Find Helpful.

[37] J. D. da Fonseca and C. V. Abud, "The Kuramoto model revisited," *J. Stat. Mech*, vol. 2018, no. 10, Article ID 103204, 13 pages, 2018.

[38] J. F. Wager, "Real- and reciprocal-space attributes of band tail states," *AIP Advances*, vol. 7, no. 12, Article ID 125321, 2017.

[39] C. Longeaud, J. Luckas, and M. Wuttig, "Some results on the germanium telluride density of states," *Journal of Physics: Conference Series*, vol. 398, Article ID 012007, 2012.

[40] Y. M. Galperin, V. G. Karpov, and V. I. Kozub, "Localized states in glasses," *Advances in Physics*, vol. 38, no. 6, pp. 669–737, 1989, eq (3.3).

[41] N. V. Dyakonova and M. E. Levinshtein, *Sov. Phys. Semicond.*vol. 23, p. 175, 1989.

[42] V. N. Abakumov, V. I. Perel, and I. N. Yassievich, *Nonradiative Recombination in Semiconductors, Modern Problems in Condensed Matter Science*, V. M. Agranovich and A. A. Maradudin, Eds., Elsevier, Amsterdam, Netherlands, 1991.

[43] W. A. Phillips, "Two-electron excitations and the low temperature properties of glasses," *Philosophical Magazine*, vol. 34, no. 6, pp. 983–991, 1976.

[44] J. C. Martinez and R. E. Simpson, "Relation between resistance drift and Optical gap in phase change materials," *Adv. Theory Simul*, vol. 3, no. 10, references therein, Article ID 2000117, 2020.

[45] A. McWhorter, "1/f noise and germanium surface properties," in *Semiconductor Surface Physics*, R. H. Kingstone, Ed., pp. 207–228, Univ. of Pensylv. Press, Philadelphia, PA, USA, 1957.

[46] V. Palenskis and K. Maknys, "Nature of low-frequency noise in homogeneous semiconductors," *Scientific Reports*, vol. 5, no. 1, Article ID 18305, 2015.

[47] J. Frenkel, "On Pre-breakdown Phenomena in Insulators and electronic semi-Conductors," *Physical Review*, vol. 54, no. 8, pp. 647-648, 1938.

[48] S. K. Bahl and K. L. Chopra, "Amorphous versus crystalline GeTe films. III. Electrical properties and band structure," *Journal of Applied Physics*, vol. 41, no. 5, pp. 2196–2212, 1970.

[49] C. Chen, P. Jost, H. Volker et al., "Physics Review B 95," *094111*, 2017.

[50] D. Adler and E. J. Yoffa, "Electronic structure of amorphous semiconductors," *Physical Review B: Condensed Matter*, vol. 36, no. 20, pp. 1197–1200, Article ID 125305, 2012.

[51] J. A. Copeland, "Semiconductor impurity analysis from low-frequency noise spectra," *IEEE Transactions on Electron Devices*, vol. 18, no. 1, pp. 50–53, 1971.

[52] Y. Ishihara, Y. Yoshita, and I. Nakada, "Specific heat of germanium monotelluride," *Journal of the Physical Society of Japan*, vol. 55, no. 6, pp. 1948–1951, 1986.

[53] K. V. Shportko, "Disorder and compositional dependences in Urbach-Martienssen tails in amorphous (GeTe)x(Sb2Te3)1−x alloys," *Scientific Reports*, vol. 9, no. 1, p. 6030, 2019.

[54] S. Datta, *Electronic Transport in Mesoscopic Systems*, Cambridge U, Press, Cambridge, UK, sec. 3.5, 1995.

[55] K. W. Clark, X. G. Zhang, G. Gu et al., "Energy gap induced by friedel Oscillations manifested as transport asymmetry at monolayer-bilayer graphene boundaries," *Phys. Rev. X*, vol. 4, no. 1, Article ID 011021, 2014.

[56] R. G. D. Jeyasingh, D. Kuzum, and H. S. P. Wong, "Investigation of trap spacing for the amorphous state of phase-change memory devices," *IEEE Trans. Electron Devices*, vol. 58, no. 12, pp. 4370–4376, 2011.

[57] H. Sakaguchi, "Cooperative phenomena in coupled oscillator systems under external fields, Progress Theory," *Physics*, vol. 79, p. 39, 1988.
[58] M. Rizzi, M. Ferro, P. Fantini, and D. Ielmini, "Energy Landscape model of conduction and phase transition in phase change memories," *IEEE Trans. Electron Devices*, vol. 60, no. 11, pp. 3618–3624, 2013.
[59] S. C. Agarwal, "Role of potential fluctuations in phase-change GST memory devices," *Phys. Status Solidi B*, vol. 249, no. 10, pp. 1956–1961, 2012.
[60] G. Liu, S. Rumyantsev, M. S. Shur, and A. A. Balandin, "Origin of 1/*f* noise in graphene multilayers: surface vs. volume," *Applied Physics Letters*, vol. 102, no. 9, Article ID 093111, 2013.
[61] R. F. Voss and J. Clarke, "Flicker (1f) noise: equilibrium temperature and resistance fluctuations," *Physical Review B: Condensed Matter*, vol. 13, no. 2, pp. 556–573, 1976.